International Journal of Chemical, Materials and Biomolecular Sciences
ISSN: 2415-6620
Vol:8, No:9, 2014

Flexible Laser Reduced Graphene Oxide/ MnO_2 Electrode for Supercapacitor Applications

Ingy N. Bkrey, Ahmed A. Moniem

***Abstract*—**We succeeded to produce a high performance and flexible graphene/Manganese dioxide (G/MnO_2) electrode coated on flexible polyethylene terephthalate (PET) substrate. The graphene film is initially synthesized by drop-casting the graphene oxide (GO) solution on the PET substrate, followed by simultaneous reduction and patterning of the dried film using carbon dioxide (CO_2) laser beam with power of 1.8 W. Potentiostatic Anodic Deposition method was used to deposit thin film of MnO_2 with different loading mass 10 – 50 and 100 μg.cm^{-2} on the pre-prepared graphene film. The electrodes were fully characterized in terms of structure, morphology, and electrochemical performance. A maximum specific capacitance of 973 F.g^{-1} was attributed when depositing 50μg.cm^{-2} MnO_2 on the laser reduced graphene oxide rGO (or G/50MnO_2) and over 92% of its initial capacitance was retained after 1000 cycles. The good electrochemical performance and long-term cycling stability make our proposed approach a promising candidate in the supercapacitor applications.

***Keywords*—**Electrode Deposition, Flexible, Graphene oxide, Graphene, High Power CO_2 Laser, MnO_2.

I. Introduction

THE current trend with portable electronics lies in continuous miniaturization, while enhancing the functionality and reliability of existing components. Flexible energy-storage devices have attracted attentions due to their potential in integration into stretchable and wearable electronics. In particular, electrochemical supercapacitors (ECs) with high power density, long cycling life, and short charging time are of significant interest as energy storage devices [1], [2]. The electrode is the key of interest in the supercapacitors fabrication, generally, the most widely used active electrode materials of supercapacitors are carbon, conducting polymers, and metal oxides[3].

Two types of ECs are available based on the charge storage mechanism. One is the electric double-layer (EDL) capacitor, which usually uses carbon-based active materials with high surface area as electrodes. The energy storing is done through the separation of electronic and ionic charges at the electrode/electrolyte interface. The second is known as pseudo-capacitors or redox supercapacitors, which is based on redox active electrode materials (e.g., metal oxides, conducting polymers) for charge storage through fast and reversible surface or near-surface Faradic reactions [2], [4], [5].

Graphene, a two-dimensional carbon sheet with monoatomic layer thickness, offers great potential for energy storage application. With graphene high theoretical surface area (2630 m^2/g) and electrical conductivity, graphene could produce supercapacitors with ultrahigh power [1]. Recently, El-Kady et al. [1], [6] developed a direct fabrication method for producing extremely thin and flexible graphene supercapacitors using a consumer-grade Light Scribe DVD burner. This process is readily scalable, and the devices can be fabricated on large substrates at a fraction of the cost of traditional micro-fabrication methods. The laser irradiation process takes about 20 min per cycle and it may take more than one cycle to perform it. Also, Strong et al. [7] proposed using DVD drive laser source to reduce and pattern of the intended GO by the modified Hummer's method and applied it over a PET substrate. In spite of the advantages of this method, the quality of the laser-reduced GO prepared by this method is low. The high intensity of the D band observed in their graphene specimen suggests that carbon sp^3 centers are still present after reduction. In addition, this process requires special sample preparation; the samples must be accurately formed as discs whose outer and inner diameters conform to the DVD standard so that they can be mounted in the DVD drive. The authors mentioned that the low quality of the produced graphene was due to insufficient reduction, a consequence of insufficient laser power, and that the quality would be improved by using a high-power laser source.

In this paper, we report the first production of a high quality flexible graphene film with minor defects, using a higher powered laser to reduce and pattern the dried graphene oxide film dispersed over a flexible PET substrate. A commercially available high power CO_2 laser printing machine was chosen, enabling reliable, fast process while using larger patterning areas and a thicker film. Furthermore, in our method, the PET substrates are simultaneously patterned and reduced, without special preparation or adjustment. In addition, the laser of the printing machine has sufficient power to allow the PET substrates to be accurately diced after reduction and patterning, which further lowers the production cost.

Meanwhile, Manganese oxide (MnO_x), has drawn considerable interest for its attractive physical and chemical properties in the electrochemical supercapacitors applications [2], [5]. In particular, manganese dioxide is recognized as one of the most promising electrode material for electrochemical

Ingy N. Bkrey is with Materials Science and Engineering Department, Egypt-Japan University of Science and Technology, New Borg El-Arab, Alexandria 21934, Egypt (corresponding author to provide phone: +201226140360; fax:4599805; e-mail: ingy.ghoniem@ejust.edu.eg).

Ahmed A. Moniem is with Materials Science and Engineering Department, Egypt-Japan University of Science and Technology, New Borg El-Arab, Alexandria 21934, Egypt, and On-leave from Physical Chemistry Department, National Research Center, Cairo 12622, Egypt (e-mail: ahmed.abdelmoneim@ejust.edu.eg).

supercapacitors because of its low-cost, good electrochemical reactivity, environmental compatibility and high performance pseudo-capacitance.[8]

Generlly, hydrated manganese oxides exhibit specific capacitances within the 100-200 $F.g^{-1}$ range in aqueous solutions. Poor electrical conductivity has been reported for micrometer-thick birnessite - type MnO_2 [9], [10]. As a result of the high charge-transfer resistance of MnO_2 electrodes, the specific capacitance and power characteristics of it are very limited. In addition, MnO_2 electrodes suffer from lack of structural stability and flexibility resulting in degraded long-term electrochemical cycle life [10]. An important consideration for alleviating the poor electronic conductivity, chemical and mechanical stabilities, and flexibility of MnO_2 electrodes is to tailor the electrode architecture via applying an ultrathin layer of MnO_2 on the surface of a porous, high surface area and electronically conducting structure to shorten the solid state transport for ions and diffusion path lengths of electrons. This can produce a good electrochemical performance without sacrificing the mass-loading of the MnO_2 phase. The porous architectures can be carbon nanofoams, template mesoporous carbon, carbon nanowires, nanotube assemblies, chitosan and conductive polymers [3], [9], [10].

In this paper, we intended the first study for the effect of various MnO_2 loading mass on the laser reduced graphene oxide via high power laser. To demonstrate the feasibility of the proposed method, the flexibility, conductivity, and electrochemical performance of the electrode had been elaborated.

II. Experimental

A. Graphene Oxide Preparations

High quality graphene oxide was synthesized from natural graphite powder (Merck KGA) by modified Hummer's method. The graphene oxide was diluted to a concentration of 3.7 $mg.mL^{-1}$ in water, and then sonicated for 1 hour, followed by centrifugation process at 3000 rpm for 20 minutes. The graphene oxide (GO) solution volume was adjusted according to the substrate dimensions (0.1413 $ml.cm^{-2}$), then the GO dispersion was drop-cast onto a thin polyethylene terephthalate (PET) substrate as shown in Fig. 1 then allowed to dry for about 48 hour.

The pre-dried graphene oxide is simultaneously reduced and patterned in one step process, into a rectangle strip of 1cm x 2cm by Universal Laser Systems VLS2.30. The program controls the carbon dioxide CO_2 (10.6 µm wave length and 30 W maximum power) laser beam, we adjusted the beam power to 1.8Watt.

B. Electrochemical Deposition of MnO_2

The electrochemical anodic deposition of MnO_2 was carried out in 0.25 M $(CH_3COO)_2Mn.4H_2O$ electrolyte at 1 V (Ag/AgCl (KCl saturated)) using Pt-wire as a counter electrode and Graphene/PET substrate as a working electrode. The mass of the deposited films was controlled by adjusting the total charge passed through the electrode during the deposition process. The estimated mass loading of the deposited MnO_2 film was 10, 50, and 100 $\mu g.cm^2$.

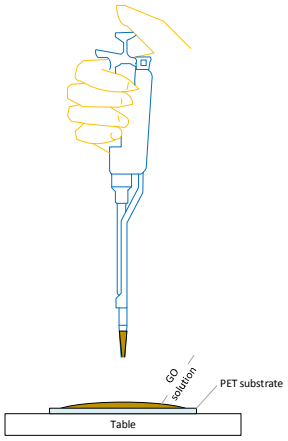

Fig. 1 Drop-casting of graphene oxide solution on PET substrate

C. Film Characterizations

Samples were characterized in terms of structure and morphology. X-ray diffraction (XRD) patterns were recorded on an X-ray diffractometer SHIMADZU, XRD-6100 by using Cu Kα radiation. Fourier transform infrared spectroscopy (FT-IR) analysis was carried out on BRUKER, VERTEX 70 Fourier transform infrared while Raman spectra were collected on an LabRAM HR-800; Horiba, (Ltd., Kyoto, Japan) laser confocal Raman spectrometer. Scanning Electron Microscopy (SEM) images were observed on JEOL JSM-6 010LV microscope. The graphene sheet resistance and conductivity values were conducted using 4-probe technique (Pro4, LUCAS LABS) taking average of 5 point per electrode.

D. Electrochemical Measurements

The cyclic voltammetry (CV), and galvanostatic charge–discharge and electrochemical impedance spectroscopy (EIS) studies were conducted on an electrochemical analyzer VeraSTAT4 (Princeton Applied Research, USA). A three-electrode system was used for all of the measurements in 0.5 M Na_2SO_4 electrolyte at room temperature with a platinum wire and an Ag/AgCl (3M KCl) as a counter and reference electrode respectively. Each working electrode was made by cutting a PET sheet coated with Graphene into rectangular pieces of the appropriate size (2*1 Cm^2). The ends were covered with conducting Copper tape to ensure good electrical contact. Part of the electrode was then covered with polyimide tape so that only a working area of 1 cm^2 was allowed to be exposed to the electrolyte as shown in Fig. 2.

The CV measurements were performed in voltage range of 0-0.9 V at scan rates of 10, 30, 50, 70, and 90 $mV.s^{-1}$. Charge/discharge measurements were carried out galvanostatically over voltage range from 0 to 1.0 V at a constant current density in the range of 0.1-0.5 $mA.cm^{-2}$.

Another concern is focused on the capacitance retention upon repeated cycling at current density of 1 $mA.cm^{-2}$ for 1000 cycles. The specific capacitance SC was calculated according to the mass of graphene and MnO_2 film. Finally,

EIS measurements were operated in a frequency range from 100K Hz to 100m Hz with AC voltage amplitude of 10 MV RMS.

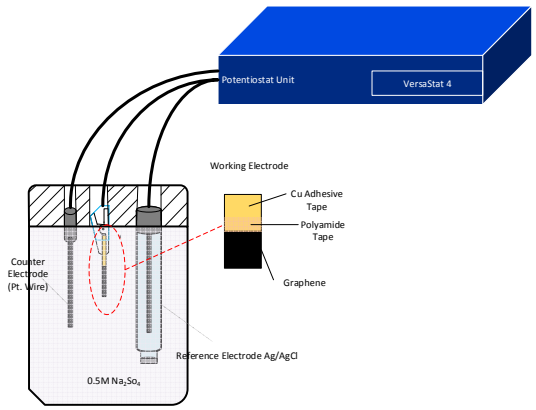

Fig. 2 Electrochemical Analysis setup and working electrode configuration

III. Results and Discussions

A. Electrode Characterizations and Morphology Study

From visual examination the change in GO color from a golden-brown into black was a direct impact of the reduction of GO into graphene [7]. In order to confirm the transformation of graphene oxide to graphene and identify its number of layers XRD, Raman, FTIR, and SEM characterizations were carried out.

The interlayer distances of Graphite, Graphene Oxide and Graphene were confirmed by XRD patterns. Fig. 3 shows the XRD patterns of graphite powder, and the deposited graphene oxide and laser-reduced graphene oxide films. A typical peak at 2θ = 26.32° corresponding to the interlayer distance (d-spacing) of 3.3937A° was observed for the graphite powder. After chemical reduction via modified Hammer method, the 2θ peak shifted to 10.54° which indicate that the graphite was fully oxidized into GO with interlayer spacing of 8.476 A° [11], [12]. In contrast, by applying a laser beam to the GO film; a narrow peak at 25.62° was observed with an estimated interlayer distance of 3.47 A° which is fairly close to that of graphite powder. This result suggesting that the GO was fully reduced into graphene film and most oxygen functional groups had been removed.

To demonstrate the vibrational properties of the samples, the Raman spectroscopy had been conducted at room temperature. Fig. 4 shows the Raman spectra of graphene and G/MnO_2 films with different MnO_2 mass. Two distinctive peaks were observed for graphene i.e. one at 1350 cm^{-1} for D band, and another at 1585 cm^{-1} for G bands. The D band is associated with the first-order Raman scattering phonon vibrational mode, while the G band assigned to sp^2 – hybridized bonded carbon atoms in two-dimensional hexagonal lattice, as well as defects [11], [13], [14]. The characteristic peaks of D band and G band have been weakened for all the G/MnO_2 films and a new characteristic peak at 630 cm^{-1} appeared suggesting the successful addition of MnO_2 on the surface of graphene sheets. [15]

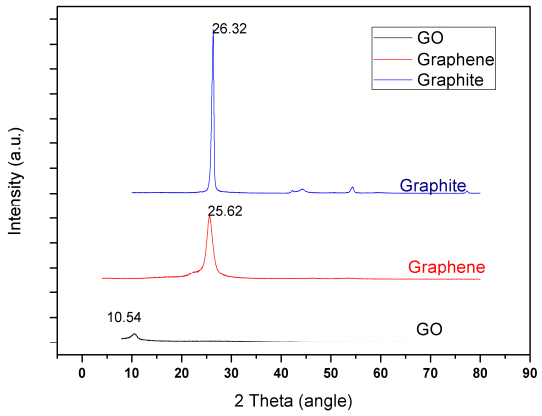

Fig. 3 XRD patterns of graphite powder, laser-reduced graphene oxide films and graphene oxide

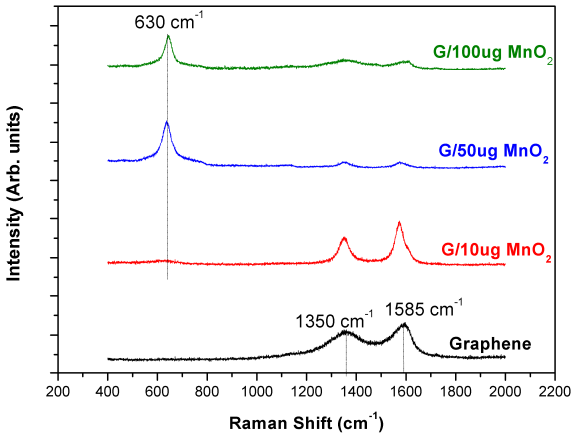

Fig. 4 Raman Spectra for Graphene and G/MnO_2 electrodes with different deposition mass

The reduction of GO was confirmed also using FT-IR spectroscopy as shown in Fig. 5. The FT-IR spectrum of the GO (Fig. 5 (a)) shows the existence of various oxygen configurations in the structure, i.e. the peak at 3435 cm^{-1} is attributed to the –O-H hydroxyl group, while the stretching vibration absorption peaks of C=O (carboxylic), C-O (epoxy), and C-O (alkoxy) are presented at 1720 cm^{-1}, 1390 cm^{-1}, and 1079 cm^{-1}respectively. The formation of hydroxyl, carboxylic, epoxy and alkoxy groups justified the recorded interlayer expansion by XRD technique after the oxidation of graphite to graphene oxide. The peak at 1629 cm^{-1} assigned to in plane C=C bands and the skeletal vibration of the graphene sheets that also confirming the successful oxidation of graphite[16]. As for the FT-IR spectrum of laser-reduced graphene oxide indicated in Fig. 5 (b) it is obvious that the characteristic absorption bands of C=O (carboxylic) and C-O (epoxy) groups was completely removed while the peaks at 1629 cm^{-1} and 1079 cm^{-1} weakened, indicating that most of GO has been successfully reduced into Graphene. All identical

characteristic vibrations peaks of G/MnO_2 film were clearly observed Fig. 5 (c), (d). Furthermore, a shoulder peak clearly observed at 520 cm^{-1} which might be corresponding to the Mn-O stretching and bending vibrations. [16]

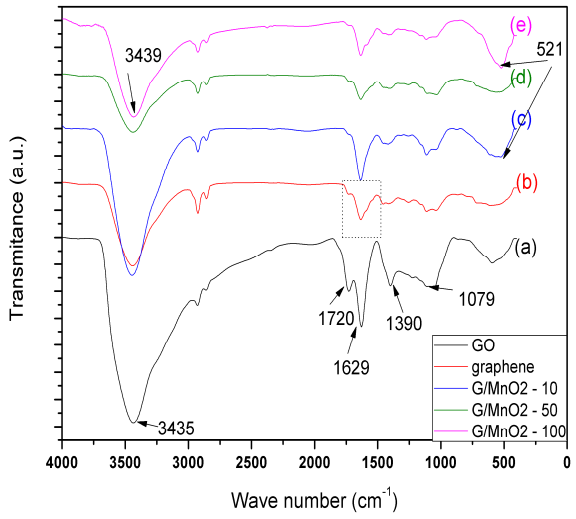

Fig. 5 FT-IR spectra of (a) GO, (b) Graphene, (c), (d), and (e) G/MnO_2 for different MnO_2 mass of 10,50, and 100 µg/cm^2 respectively

Fig. 6 presents a cross-sectional SEM image of the film at the interface between GO and laser reduced graphene shows the expansion of the film after treatment with the laser.

Fig. 7 presents SEM images of (a) Graphene free MnO_2 electrode at higher magnification, (b)-(d) G/MnO_2 electrodes with different MnO_2 mass of loading where (b) G/10MnO_2, (c) G/50MnO_2, and (d) G/100MnO_2. Fig. 7 (a) shows that the graphene maintains its structure morphology at high magnification proving that reduction with laser of GO forms a three-dimensional network of overlapped graphene flakes with possible highly accessible surface area [1], making this method one of the best choices for electrochemical supercapacitor applications. The deposition process of MnO_2 on the laser rGO was included in Fig. 7 (b)-(d) showing the effect of increasing MnO_2 mass loaded on it. With 10µg.cm^{-2} MnO_2 mass (G/10MnO_2) (Fig. 7 (a)), MnO_2 only partially distributed along the structure, leaving the graphene clearly observed. At increased deposition mass 50-100 µg.$cm^{-2}$$MnO_2$ (Fig. 7 (b), (c)), much more MnO_2 was deposited along the graphene structure. At Fig. 7 (c) the MnO_2 mass clog the porous graphene structure leaving crack like structure, which in turn have direct impact on the degree of flexibility and the performance of Electrochemical Suppercapacitor.

The laser reduction process results in the removal of oxygen species and the re-form of the sp^2 carbons [7]. This causes a change in the conductivity of the film from the insulating graphite oxide, with a typical resistance of >20 MΩ/sq to highly conducting graphene. The electrodes show excellent conductivity of about 237 S/m using the 4-probe technique.

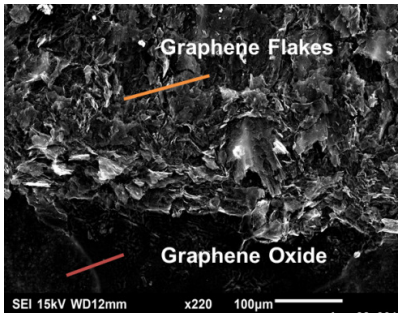

Fig. 6 Cross-sectional SEM image of the film at the interface between GO and graphene (Magnification 100µm)

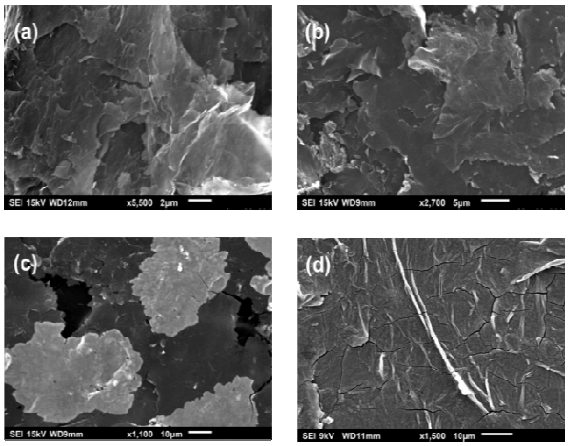

Fig. 7 SEM images of (a) Graphene free MnO_2 electrode at high magnification, (b-d) G/MnO_2 electrodes with different MnO_2 mass of loading at (b) G/10MnO_2, (c) G/50MnO_2, and (d) G/100MnO_2

B. Electrochemical Supercapacitive Behavior

1. Cyclic Voltammetry

The capacitance performance of the laser reduced graphene oxide (rGO) and the G/MnO_2 composite films were explored using Cyclic Voltammetry. Since MnO_2 suffers from lack of stability above ca. 1.0V [2], we examined the CV of the electrode at a potential of 0 – 0.9 V. Fig. 8 shows the CV performance for laser rGO and G/MnO_2 electrodes. It is apparently noticed that in Fig. 8 (a)-(c) the curves are almost ideally rectangular-shaped and symmetric which considered a sign on the fast reversible redox reaction and a typical capacitive behavior of the electrodes. However, with increasing the mass of deposited Manganese Oxide to 100µg.cm^{-2} (Fig. 8 (d)) the curve deviated from rectangular shape to some extent. This could be due to the decrease of the effective interaction between electrolyte and electrode which limit the utilization of laser rGO electrodes.

2. Galvanostatic Charge / Discharge Characteristic

In order to evaluate the effect of MnO_2 loading over laser rGO on the capacitive behavior and rate capability, the charge and discharge experiments were carried out by potentiosat4.

Fig. 9 presents charge–discharge profiles of G/MnO_2 electrodes with different manganese dioxide mass content at current density of 0.1 mA.cm^{-2}. The inset presents the charge–

discharge profile for graphene.

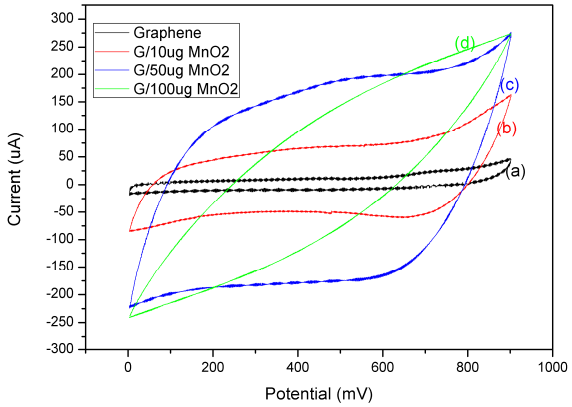

Fig. 8 CV curves for (a) graphene free MnO_2, and G/MnO_2 electrodes at different loading mass (b) 10µg.cm^{-2}, (c) 50µg.cm^{-2}, and (d) 100µg.cm^{-2}, at scan rate of 10mV/s

In principle, the discharge profile of any oxide film with capacitive characteristics is basically consisted of three parts: First, The voltage drop at the beginning of each discharge curve which known as the IR drop, is a measure of the overall resistance of the device, and as its value is attributed to the discharge current. Second, the capacitance component corresponding to the voltage change due to ion separation in the double layer region at the electrode interface, and finally faradaic component in the longer time region due to charge transfer reaction of the film [9], [17].

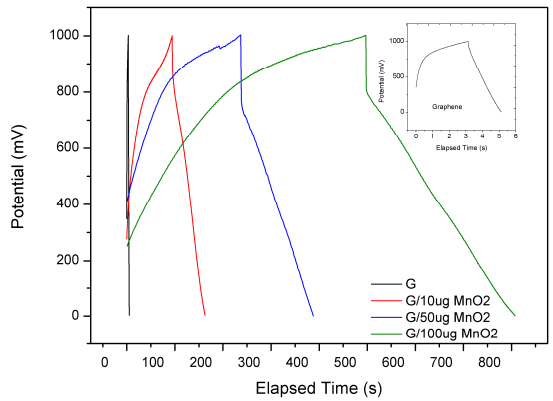

Fig. 9 Galvanostatic charge/discharge curves of G/MnO_2 electrodes at constant current desnity of 0.1 mA.Cm^{-2}. The insert is the galvanostatic charge/discharge curve for graphene

Demonstrably, from Fig. 9 it could be denoted that the charge curves are almost symmetric with a slight curvature to their corresponding discharge counterparts, confirming the fine cycling stability and the reversible performance. Furthermore, the discharge time for G/100MnO_2 is much higher than other electrode configurations suggesting the capacitive behavior of the electrode; because the discharge time is directly proportional to specific capacitance.

The specific capacitance from discharge curves can be calculated from the following equation [12]

$$SC = \frac{I}{m \cdot \frac{\Delta v}{\Delta t}} \quad (1)$$

where SC is the specific capacitance (F.g^{-1}), I is the charge/discharge current, $\Delta v/\Delta t$ is the slope of the discharge curve, and m is mass of the active material within the electrode. Fig. 10 shows the capacitance performance in 0.1 – 0.5 mA.cm^{-2} current density range for different electrode configurations. The highest specific capacitance was 1907, 973, 382, and 11 F.g^{-1} for G/100MnO_2, G/50MnO_2, G/10MnO_2, and Graphene, respectively at 0.1 mA.cm^{-2} current density. Also, it could be seen that as the charging current increased, the charging process became more difficult due to limited migration of ions in electrode exhibiting a decrease in the specific capacitance values[18].

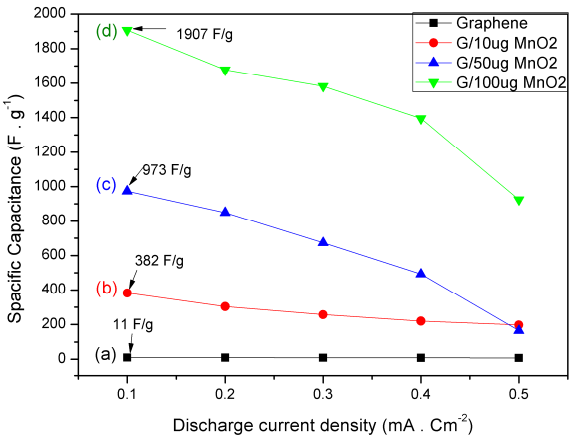

Fig. 10 Specific Capacitance vs. discharge current density for (a) Graphene, (b) G/10MnO_2, (c) G/50MnO_2, and(d) G/100MnO_2

3. Galvanostatic Charge-Discharge & Cyclic Stability

Long-term cycling stability of the fabricated solid-state device was also examined by galvanostatic charge–discharge cycling at a current density of 1mA.cm^{-2}. Fig. 11 shows the capacitance retention of G/MnO_2 electrodes as a function of cycle number. Significantly, G/50MnO_2 electrode exhibits an excellent long-term stability without fluctuations, which maintain about 99% from its initial capacitance for the first 900 cycles then down to 92.2% retention after 1000 cycles. This could be fine indication about electro-activation as well as long term electro-chemical and mechanical cycling stabilities.[19]

4. Electrochemical Impedance Spectroscopy

To evaluate the validity of our developed laser rGO and G/MnO_2 composite films to operate as electrodes for supercapacitor applications, the electrochemical impedance measurements were carried out. The ideal Nquist plot contains a half semi-circle and a straight line at low frequency. The Nquist impedance plot for Graphene and G/MnO_2 composite electrodes is shown in Fig. 12. A similar behavior appeared for all curves composed of a high frequency arc followed by a

low frequency line. At very high frequency region, the intercept with the real axis (Z') provides equivalent series resistance ESR, which includes the resistance of the electrolyte, the intrinsic resistance of the active material, and the contact resistance at the interface between active material, electrolyte and current collector [18]-[20].

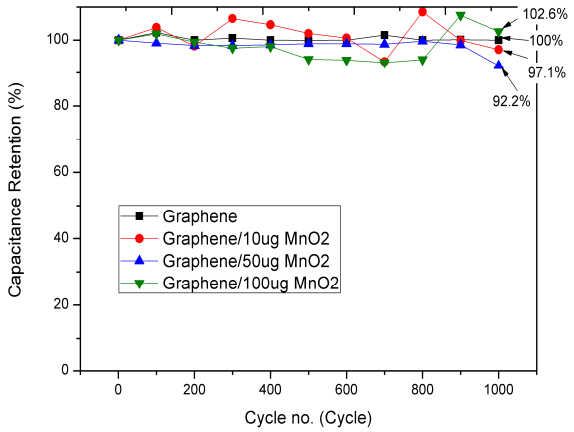

Fig. 11 Capacitance stability retention at current density of 1mA.cm^{-2} and 1000 cycles for Graphene & G/MnO_2 composite electrodes

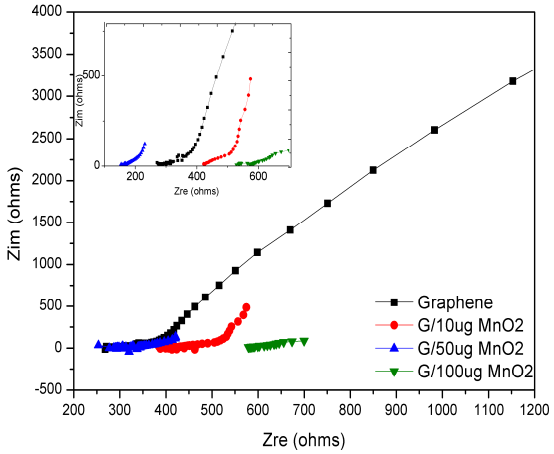

Fig. 12 Nquist plot for Graphene and G/MnO_2 electrodes with different loading mass, the insert is the expanded view in the high frequency region

The insert in Fig. 12 shows the high frequency region of the Nquist plot denoting that the ESR for Graphene, G/10 MnO_2, G/50 MnO_2 and G/100 MnO_2 is 169Ω, 385Ω, 102Ω, and 528Ω respectively. Obviously, the ESR for G/50 MnO_2 composite electrode is the lowest which has a direct impact on the improvement of the electrode performance. The diameter of the high frequency arc corresponds to the real impedance such as ionic charge-transfer resistance R_{ct} of the composite layer in electrode. It can be seen from Fig. 12 that the smallest R_{ct} was for G/50 MnO_2 which is beneficial to facilitate charge-transfer process and for the migration of ions [12].

The capacitive behavior of the electrode is determined by the imaginary part of the impedance at low frequency region and it should approaches a 90° vertical line in an ideal capacitor. In the impedance plot in Fig. 12 there is a deviation in the curve from vertical line which may be attributed to high porosity, low mobility of protons inside the electrode of combination between these factors [20].

IV. Conclusions

We proposed and verified a new fabrication technique for producing patterned multilayer graphene films on large flexible PET substrates using a cost-effective approach. In this method, GO was prepared by a modified Hummers method then drop casted on flexible PET substrate. The pre-dried graphene oxide film is then subjected to simultaneous reduction and patterning using laser carbon dioxide beam. The proposed method is simple, economical, and suited for mass production. Anodic deposition was used to load different MnO_2 mass on the flexible pre-prepared graphene. Electrode characterizations show that the increase in MnO_2 mass has a direct impact on the morphology and electrochemical performance of the electrode. The electrochemical performance of laser reduce graphene oxide electrode was enhanced by loading MnO_2 with less than 100μg/cm^2 mass. Although, there is an increase in the charge-discharge SC value to 1907 F.g^{-1} for G/100MnO_2 electrode, the electrode flexibility decay in addition to its capacitive behavior. We could deduce that the best electrode configuration was for G/50MnO_2 electrode from CV results, Impedance, and cyclic stability point of view. The highest obtained charge-discharge SC value was 973 F.g^{-1}at 0.1mA.cm^{-2} for G/50MnO_2 electrode. The specific capacitance of the electrode exhibit excellent stability during 1000 cycles at a current density of 1mA.cm^{-2}. The excellent capacitive behavior shows that the amorphous MnO_2 films with laser reduced graphene oxide can be an excellent candidate as electrode material for supercapacitors.

Acknowledgment

The authors gratefully acknowledge the Missions Sector-Higher Education Ministry, Egypt for financial support through this work, Materials Science and Engineering Department at E-JUST, and Japan International Cooperation Agency (JICA) for their supports through this work.

References

[1] M. F. El-Kady and R. B. Kaner, "Scalable fabrication of high-power graphene micro-supercapacitors for flexible and on-chip energy storage.," *Nat. Commun.*, vol. 4, p. 1475, Jan. 2013.
[2] Q. Chen, Y. Meng, C. Hu, Y. Zhao, H. Shao, N. Chen, and L. Qu, "MnO2-modified hierarchical graphene fiber electrochemical supercapacitor," *J. Power Sources*, vol. 247, pp. 32–39, Feb. 2014.
[3] Z. Li, Y. Mi, X. Liu, S. Liu, S. Yang, and J. Wang, "Flexible graphene/MnO2 composite papers for supercapacitor electrodes," *J. Mater. Chem.*, vol. 21, no. 38, p. 14706, 2011.
[4] S. Shi, C. Xu, C. Yang, J. Li, H. Du, B. Li, and F. Kang, "Flexible supercapacitors," *Particuology*, vol. 11, no. 4, pp. 371–377, Aug. 2013.
[5] G. Wang, L. Zhang, and J. Zhang, "A review of electrode materials for electrochemical supercapacitors.," *Chem. Soc. Rev.*, vol. 41, no. 2, pp. 797–828, Jan. 2012.

[6] M. F. El-Kady, V. Strong, S. Dubin, and R. B. Kaner, "Laser scribing of high-performance and flexible graphene-based electrochemical capacitors.," *Science*, vol. 335, no. 6074, pp. 1326–30, Mar. 2012.
[7] V. Strong, S. Dubin, M. F. El-Kady, A. Lech, Y. Wang, B. H. Weiller, and R. B. Kaner, "Patterning and electronic tuning of laser scribed graphene for flexible all-carbon devices.," *ACS Nano*, vol. 6, no. 2, pp. 1395–403, Mar. 2012.
[8] Y. J. Kang, H. Chung, and W. Kim, "1.8-V flexible supercapacitors with asymmetric configuration based on manganese oxide, carbon nanotubes, and a gel electrolyte," *Synth. Met.*, vol. 166, pp. 40–44, Feb. 2013.
[9] S. Hassan, M. Suzuki, S. Mori, and A. A. El-Moneim, "MnO2/carbon nanowalls composite electrode for supercapacitor application," *J. Power Sources*, vol. 249, pp. 21–27, Mar. 2014.
[10] W. Wei, X. Cui, W. Chen, and D. G. Ivey, "Manganese oxide-based materials as electrochemical supercapacitor electrodes.," *Chem. Soc. Rev.*, vol. 40, no. 3, pp. 1697–721, Mar. 2011.
[11] G. Han, Y. Liu, E. Kan, J. Tang, L. Zhang, H. Wang, and W. Tang, "Sandwich-structured MnO2/polypyrrole/reduced graphene oxide hybrid composites for high-performance supercapacitors," *RSC Adv.*, vol. 4, no. 20, p. 9898, 2014.
[12] K. S. B. De Silva, S. Gambhir, X. L. Wang, X. Xu, W. X. Li, D. L. Officer, D. Wexler, G. G. Wallace, and S. X. Dou, "The effect of reduced graphene oxide addition on the superconductivity of MgB2," *J. Mater. Chem.*, vol. 22, no. 28, p. 13941, 2012.
[13] B. Mu, W. Zhang, S. Shao, and A. Wang, "Glycol assisted synthesis of graphene-MnO2-polyaniline ternary composites for high performance supercapacitor electrodes.," *Phys. Chem. Chem. Phys.*, vol. 16, no. 17, pp. 7872–80, May 2014.
[14] P. Cui, J. Lee, E. Hwang, and H. Lee, "One-pot reduction of graphene oxide at subzero temperatures.," *Chem. Commun. (Camb).*, vol. 47, no. 45, pp. 12370–2, Dec. 2011.
[15] X. Huang, N. Hu, R. Gao, Y. Yu, Y. Wang, Z. Yang, E. Siu-Wai Kong, H. Wei, and Y. Zhang, "Reduced graphene oxide–polyaniline hybrid: Preparation, characterization and its applications for ammonia gas sensing," *J. Mater. Chem.*, vol. 22, no. 42, p. 22488, 2012.
[16] K.-J. Huang, D.-J. Niu, J.-Y. Sun, C.-H. Han, Z.-W. Wu, Y.-L. Li, and X.-Q. Xiong, "Novel electrochemical sensor based on functionalized graphene for simultaneous determination of adenine and guanine in DNA.," *Colloids Surf. B. Biointerfaces*, vol. 82, no. 2, pp. 543–9, Feb. 2011.
[17] M. D. Stoller and R. S. Ruoff, "Best practice methods for determining an electrode material's performance for ultracapacitors," *Energy Environ. Sci.*, vol. 3, no. 9, p. 1294, 2010.
[18] D. P. Dubal and R. Holze, "All-solid-state flexible thin film supercapacitor based on Mn3O4 stacked nanosheets with gel electrolyte," *Energy*, vol. 51, pp. 407–412, Mar. 2013.
[19] Y. Zhang, G. Li, Y. Lv, L. Wang, A. Zhang, Y. Song, and B. Huang, "Electrochemical investigation of MnO2 electrode material for supercapacitors," *Int. J. Hydrogen Energy*, vol. 36, no. 18, pp. 11760–11766, Sep. 2011.
[20] B. E. Conway, "Electrochemical Supercapacitors Scientific Fundamentals and Technological Applications." , pp.525-55, 1999.